

# Dynamical screening of the Coulomb interaction for two confined electrons in a magnetic field

N. S. Simonović<sup>1</sup> and R. G. Nazmitdinov<sup>2,3</sup>

<sup>1</sup>*Institute of Physics, P.O. Box 57, 11001 Belgrade, Serbia*

<sup>2</sup>*Departament de Física, Universitat de les Illes Balears, E-07122 Palma de Mallorca, Spain*

<sup>3</sup>*Bogoliubov Laboratory of Theoretical Physics, Joint Institute for Nuclear Research, 141980 Dubna, Russia*

(Dated: September 15, 2021)

We show that a difference in time scales of vertical and lateral dynamics permits one to analyze the problem of interacting electrons confined in an axially symmetric three-dimensional potential with a lateral oscillator confinement by means of the effective two-dimensional Hamiltonian with a screened Coulomb interaction. Using an adiabatic approximation based on action-angle variables, we present solutions for the effective charge of the Coulomb interaction (screening) for a vertical confinement potential simulated by parabolic, square, and triangular wells. While for the parabolic potential the solution for the effective charge is given in a closed analytical form, for the other cases similar solutions can be easily calculated numerically.

PACS numbers: 03.65.Sq, 31.15.xg, 73.21.La

## I. INTRODUCTION

It is well known that there is a restricted class of exactly solvable problems in quantum mechanics. Such examples serve as paradigms to illustrate fundamental principles or/and new methods in their respective fields. This is especially important for finite systems, where approximative methods are indispensable to a many-body problem. In particular, two-electron systems play an important role in understanding of electron correlation effects because their eigenstates can be obtained very accurately, or in some cases, exactly.

The most popular model to study the electronic exchange-correlation energy in a density functional theory is the Hookean two-electron atom (HA). The basic HA is two electrons interacting by the Coulomb potential but bound to a nucleus by a harmonic potential that mimics a nuclear-electron attraction. For certain values of the confinement strength, there exist exact solutions for the HA ground state [1, 2]. When the HA is placed in a perpendicular magnetic field, Taut provided analytical solutions for a two-dimensional (2D) HA at particular values of the magnetic field [3]. This model can be equally viewed as a model 2D quantum dot (QD). Recent progress in semiconductor technology made it possible to fabricate and probe such confined system at different values of the magnetic field [4, 5]. Consequently, it has stimulated numerous theoretical studies on two-electron QDs, so-called "artificial atoms" (see for a recent review [6]). Being a simple nontrivial system, QD He poses a significant challenge to theorists. For example, using a 2D He QD model, one is able to reproduce a general trend for the first singlet-triplet (ST) transitions observed in two-electron QDs under a perpendicular magnetic field. However, the experimental positions of the ST transition points are systematically higher [5, 7]. The ignorance of the third dimension is the most evident source of the disagreement, especially, in vertical QDs [8, 9, 10].

Although accurate numerical results for QD He can be obtained readily, analytical results are still sought, because they provide the physical insight into numerical calculations. Moreover, analytical results could establish a theoretical framework for accurate analysis of confined many-electron systems, where the exact treatment of the three-dimensional (3D) case becomes computationally intractable. The purpose of the present paper is to introduce a consistent approach which enables one to reduce the 3D Coulomb problem to the effective 2D one, without losing major effects related to the QD's thickness. In Section II we develop the concept of the effective charge of the Coulomb potential based on the adiabatic approximation [11] for axially symmetric 3D systems. The calculations of the effective charge for a Hamiltonian with a vertical confinement approximated by parabolic, square, and triangular well potentials are presented in Section III. Finally, we will show in Section IV that recent experimental data [7] can be successfully reproduced within a 2D approximation but with additionally screened Coulomb interaction due to the thickness of the sample. The main outcomes are summarized in Section V. Three Appendixes provide some technical details of the calculations.

## II. BASIC REMARKS

### A. Model

The system Hamiltonian for the case of a magnetic field  $B$  along a symmetry axis  $z$  reads

$$H = \sum_{i=1}^2 \left[ \frac{1}{2m^*} \left( \mathbf{p}_i - \frac{e}{c} \mathbf{A}_i \right)^2 + U(\mathbf{r}_i) \right] + V_C + H_{spin}. \quad (1)$$

Here the term  $V_C = k/|\mathbf{r}_1 - \mathbf{r}_2|$  with  $k = e^2/4\pi\epsilon_0\epsilon_r$  describes the Coulomb repulsion between electrons and

$H_{spin} = g^* \mu_B (\mathbf{s}_1 + \mathbf{s}_2) \mathbf{B}$  is the Zeeman term, where  $\mu_B = |e| \hbar / 2m_e c$  is the Bohr magneton. For the magnetic field we choose the vector potential with gauge  $\mathbf{A}_i = \frac{1}{2} \mathbf{B} \times \mathbf{r}_i = \frac{1}{2} B (-y_i, x_i, 0)$ . The confining potential is approximated by a 2D circular harmonic oscillator (HO) in  $xy$ -plane and the vertical confinement  $V_z$ :  $U(\mathbf{r}_i) = m^* \omega_0^2 \rho_i^2 / 2 + V_z(z_i)$ ;  $r_i^2 = \rho_i^2 + z_i^2$ ,  $\rho_i^2 = x_i^2 + y_i^2$  and  $\hbar \omega_0$  is the energy scale of confinement in the  $xy$ -plane. Below we analyze different forms for the vertical confinement  $V_z$ .

For our analysis it is convenient to use cylindrical coordinates  $(\rho, \phi, z)$ . Also, we separate the Hamiltonian (1) on several terms:  $H = H_0 + H_z + V_C + H_{spin}$ , where the term  $H_0 = \sum_{i=1}^2 h_i$  consists of the contributions related only to the lateral dynamics ( $xy$ -plane) of non-interacting electrons

$$h_i = t_i + v_i - \omega_L l_{z_i} = \frac{p_{\rho_i}^2}{2m^*} + \left( \frac{l_{z_i}^2}{2m^* \rho_i^2} + \frac{1}{2} m^* \Omega^2 \rho_i^2 \right) - \omega_L l_{z_i}. \quad (2)$$

Here, the effective lateral confinement frequency  $\Omega = (\omega_0^2 + \omega_L^2)^{1/2}$  depends on the magnetic field by means of the Larmor frequency  $\omega_L = |e| B / 2m^* c$ ;  $l_{z_i} \equiv p_{\phi_i}$  is the  $z$ -component of the angular momentum of the  $i$ -th electron. The eigenstates of the single-particle Hamiltonian (2) are well-known Fock-Darwin states (cf [12]). The motion of noninteracting electrons in the  $z$ -direction is described by the Hamiltonian  $H_z = \sum_i (p_{z_i}^2 / 2m^* + V_z(z_i))$ . Since the magnetic field is directed along the  $z$  axis, the Zeeman term is  $H_{spin} = g^* \mu_B S_z B$ . This term is not important for our analytical study and will be taken into account only in numerical analysis of experimental data.

## B. Adiabatic approximation

For typical QDs ( $\hbar \omega_0 \sim 3$  meV) the contribution of the Coulomb interaction to the total energy is comparable to the confinement energy at zero magnetic field [5]. Evidently, the standard perturbation theory is not valid in this case. In real samples the confining potential in the  $z$ -direction is much stronger than in the  $xy$ -plane. It results in different time scales (see below) and this allows one to use the adiabatic approach [11]. To lowest order the adiabatic approach consists of averaging the full 3D Hamiltonian over the angle variables  $\theta_{z_i} = \omega_{z_i} t$  (fast variables) of the unperturbed motion ( $k = 0$ ) after rewriting the  $(z_i, p_{z_i})$  variables in terms of the action-angle variables  $(J_{z_i}, \theta_{z_i})$ . As a result, the motion effectively decouples into an unperturbed motion in the vertical direction governed by the potential  $\sum_i V(J_{z_i}, \theta_{z_i})$  and into the lateral motion governed by the effective potential

$$V_{\text{eff}}(\{x, y\}; \{J_z\}) = \sum_i v_i + V_{\text{int}}^{\text{eff}}(\rho; J_{z_1}, J_{z_2}), \quad (3)$$

where  $v$  is defined in Eq.(2),  $\rho = [(x_1 - x_2)^2 + (y_1 - y_2)^2]^{1/2}$ , and

$$V_{\text{int}}^{\text{eff}}(\rho; J_{z_1}, J_{z_2}) = \frac{1}{(2\pi)^2} \int_0^{2\pi} d\theta_{z_1} \int_0^{2\pi} d\theta_{z_2} V_C(\rho, z_1(J_{z_1}, \theta_{z_1}) - z_2(J_{z_2}, \theta_{z_2})) \quad (4)$$

is the effective electron-electron interaction that contains the memory on  $z$  dynamics through integrals of motion  $J_{z_i}$ . The effective interaction affects, therefore, only the dynamics in the lateral plane, where the confining potential is the parabolic one (see Eq.(2)). Hence, the effective Hamiltonian for two-electron QD reads as

$$H_{\text{eff}} = H_0 + E_z + V_{\text{int}}^{\text{eff}}, \quad (5)$$

where  $E_z = \sum_i \varepsilon_i$  and  $\varepsilon_i$  is the electron energy of the unperturbed motion in the vertical direction.

Our *ansatz* consists in the consideration of the effective interaction (4) in the form  $V_{\text{int}}^{\text{eff}} = k f(\rho) / \rho$ . Then one can define the effective 2D Coulomb interaction

$$V_C^{\text{eff}} = \frac{k_{\text{eff}}}{\rho}, \quad (6)$$

where the effective charge is the mean value of the factor  $f(\rho)$  upon the nonperturbed lateral wave functions, i.e.,

$$k_{\text{eff}} = k \langle f(\rho) \rangle \equiv \langle \rho V_{\text{int}}^{\text{eff}}(\rho) \rangle. \quad (7)$$

In contrast to a standard 2D consideration of the bare Coulomb potential ( $V_C = k/\rho$ ) in QDs [5, 6], in our approach the electron dynamics is governed by the same potential but with the additional effective (screened) charge due to the QD's thickness. One of the main advantages of this approach is that the interaction matrix elements can be expressed in an analytical form. Thus, we shall use (diagonalize) the effective Hamiltonian (5) with the effective Coulomb interaction  $V_C^{\text{eff}}$ , i.e.,  $V_{\text{int}}^{\text{eff}} \Rightarrow V_C^{\text{eff}}$ .

According to the Kohn theorem [14] the center of mass (CM) and the relative motion of the 2D system described by the Hamiltonian (5) are separated and the mean value in Eq.(7) can be evaluated using the Fock-Darwin states for the relative motion

$$\psi_{n_\rho m}(\rho, \varphi) = \frac{e^{im\varphi}}{\sqrt{2\pi}} R_{n_\rho m}(\rho). \quad (8)$$

This state is eigenfunction of the operator  $l_z$  with eigenvalue  $m$  and the radius-dependent function with a radial quantum number  $n_\rho$  has the form

$$R_{n_\rho m}(\rho) = \sqrt{\frac{2\mu\Omega n_\rho!}{\hbar(n_\rho + |m|)!}} \xi^{|m|} e^{-\xi^2/2} L_{n_\rho}^{|m|}(\xi^2), \quad (9)$$

where  $\mu = m^*/2$  is the reduced mass,  $\xi = (\mu\Omega/\hbar)^{1/2} \rho$  and  $L_{n_\rho}^{|m|}$  denotes the Laguerre polynomials [13]. For the lowest states (with different values of the quantum number  $m$  but with the radial quantum number  $n_\rho = 0$ ) one obtains for the effective charge

$$k_{\text{eff}} = \frac{2}{|m|!} \left( \frac{\mu\Omega}{\hbar} \right)^{|m|+1} \int_0^\infty e^{-\mu\Omega\rho^2/\hbar} \rho^{2|m|+2} V_{\text{int}}^{\text{eff}}(\rho) d\rho. \quad (10)$$

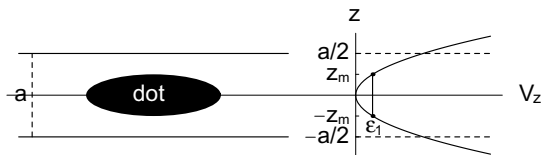


FIG. 1: Left: the localization of QD in the layer of the thickness  $a$ . Right: the schematic representation of the position of zero-point motion in the parabolic confinement relative to the layer thickness.

### III. EFFECTIVE CHARGE

#### A. Parabolic potential

To account for effect of localization of the dot in the layer of thickness  $a$ , let us first consider a 3D model with a vertical confinement approximated by a parabolic potential  $V_z(z_i) = \frac{1}{2} m^* \omega_z^2 z_i^2$  (see Fig. 1). Due to the Kohn theorem [14] the CM and the relative motions are separated. The solution for the CM motion is well known (cf [12]). It is not important for our discussion, since the CM dynamics does not affect the electron interaction. The 3D Hamiltonian for the relative motion of two electrons has the form

$$H_{\text{rel}} = h_{\text{rel}} + \frac{k}{r} + \frac{p_z^2}{2\mu} + \frac{\mu\omega_z^2 z^2}{2}. \quad (11)$$

The term  $h_{\text{rel}}$  is defined by Eq.(2) in which the effective electron mass is replaced by the reduced mass  $\mu$ ; all single-electron variables (with index  $i$ ) are replaced by the corresponding variables for relative motion (without indices).

After rewriting the  $(z, p_z)$  variables in terms of the action-angle variables  $(J_z, \theta_z)$

$$z = \sqrt{\frac{2J_z}{\mu\omega_z}} \sin \theta_z, \quad p_z = \mu \dot{z}, \quad (12)$$

we integrate out of the fast variable, i.e., average the Hamiltonian (11) over the angle  $\theta_z$ . As a result, the effective interaction potential (see also Appendix A) is

$$V_{\text{int}}^{\text{eff}}(\rho; J_z) = \frac{2k}{\pi\rho} K\left(-\frac{2J_z}{\mu\omega_z\rho^2}\right), \quad (13)$$

where  $K(x) = \int_0^{\pi/2} (1 - x \sin^2 \theta)^{-1/2} d\theta$  is the complete elliptic integral of the first kind (see [15]). This integral is well defined for all values of  $\rho$ .

The effective Hamiltonian for the relative motion is

$$H_{\text{rel}}^{\text{eff}} = h_{\text{rel}} + V_{\text{int}}^{\text{eff}}(\rho; J_z) + E_z^{\text{rel}} \quad (14)$$

$$E_z^{\text{rel}} = \omega_z J_z = \hbar\omega_z(n_z + 1/2). \quad (15)$$

To replace the effective electron-electron potential  $V_{\text{int}}^{\text{eff}}$  by the Coulomb-type  $V_C^{\text{eff}}$  in Eq.(14), we must determine the effective charge. Taking into account the definitions Eqs.(7), (15) and the result Eq.(13), one obtains the following for the effective charge

$$k_{\text{eff}} = \frac{2k}{\pi} \left\langle n_\rho, m \left| K\left(-\frac{\hbar(2n_z + 1)}{\mu\omega_z\rho^2}\right) \right| n_\rho, m \right\rangle, \quad (16)$$

where  $|n_\rho, m\rangle$  are the Fock-Darwin states for the relative motion, Eqs. (8),(9).

For the lowest states ( $n_\rho = n_z = 0$ ) one reduces Eq.(16) to the form of integral (10). As a result, the effective charge can be expressed in terms of the Meijer G-function [16]

$$k_{\text{eff}} = \frac{k}{\pi|m|!} G_{2,3}^{2,2}\left(\frac{\Omega}{\omega_z} \left| \begin{matrix} 1/2 & 1/2 \\ 0 & m+1 & 0 \end{matrix} \right. \right). \quad (17)$$

Guided by the adiabatic approach, it is instructive to compute the effective charge by dint of quantum-mechanical mean value of the Coulomb term in the 3D oscillator state  $|n_\rho, m\rangle|n_z\rangle$

$$k_{\text{eff}} = \langle\langle \rho V_C(\rho, z) \rangle\rangle = k \langle\langle (1 + z^2/\rho^2)^{-1/2} \rangle\rangle. \quad (18)$$

Here,  $|n_z\rangle$  is a normalized one-dimensional harmonic oscillator wave function [13]. Since the lateral extension exceeds the thickness of the QDs by several times, one may suggest to consider the ratio  $(z/\rho)^2$  as a small parameter of theory. Note, however, that the averaging over the 3D oscillator state  $|n_\rho, m\rangle|n_z\rangle$  implies the application of the first order perturbation theory for calculation of the contribution of the Coulomb interaction in QDs. For  $n_\rho = n_z = 0$  one obtains

$$k_{\text{eff}} = k \frac{2}{|m|!} \left(\frac{\mu\Omega}{\hbar}\right)^{|m|+1} \sqrt{\frac{\mu\omega_z}{\pi\hbar}} \int_0^\infty K_0\left(\frac{\mu\omega_z\rho^2}{2\hbar}\right) e^{\mu(\frac{1}{2}\omega_z - \Omega)\rho^2/\hbar} \rho^{2|m|+2} d\rho, \quad (19)$$

where  $K_0$  is the modified Bessel function of the 2nd kind. One observes that in both definitions of the ef-

fective charge Eqs.(16),(19) there is a contribution of the electron dynamics along the coordinate  $z$ . Below we will

compare true contogion of both definitions upon the interpretation of the experimental data.

For small and relatively large values of the magnetic

field  $0 < \Omega/\omega_z < 1$ , available in experiment, the solution for the last integral can be expressed in terms of the hypergeometric functions

$$k_{\text{eff}} = k \frac{2^{2|m|+1}}{\sqrt{\pi}|m|!} \left(\frac{\Omega}{\omega_z}\right)^{|m|+1} \left[ \Gamma\left(\frac{2|m|+3}{4}\right)^2 {}_2F_1\left(\frac{2|m|+3}{4}, \frac{2|m|+3}{4}, \frac{1}{2}, \left(1-2\frac{\Omega}{\omega_z}\right)^2\right) + 2\left(1-2\frac{\Omega}{\omega_z}\right) \Gamma\left(\frac{2|m|+5}{4}\right)^2 {}_2F_1\left(\frac{2|m|+5}{4}, \frac{2|m|+5}{4}, \frac{3}{2}, \left(1-2\frac{\Omega}{\omega_z}\right)^2\right) \right]. \quad (20)$$

### B. Infinite square well

A hard wall potential is among popular models for the confinement in QDs. In case of the vertical confinement,  $V_z$  is the one-dimensional infinite square well

$$V_z = \begin{cases} 0, & |z| < a/2 \\ \infty, & |z| \geq a/2 \end{cases}, \quad (21)$$

where  $a$  is the thickness of the layer in which the dot is created (see Fig. 1).

Due to uniform motion inside the square well, the angle variable  $\theta_{z_i}$  is proportional to the coordinates  $z_i$  (see Eq. (B3) in Appendix B) and, therefore,

$$V_{\text{int}}^{\text{eff}} = \frac{1}{\pi^2} \int_{-\pi/2}^{\pi/2} d\theta_{z_1} \int_{-\pi/2}^{\pi/2} d\theta_{z_2} V_C(\rho, z) \\ = \frac{k}{a^2} \int_{-a/2}^{a/2} dz_1 \int_{-a/2}^{a/2} dz_2 [\rho^2 + (z_1 - z_2)^2]^{-1/2}. \quad (22)$$

Integrating over the coordinates  $z_1$  and  $z_2$  between the walls of the potential (21) one obtains the effective Coulomb interaction  $V_{\text{int}}^{\text{eff}} = k\mathcal{A}(\xi)/a$ , where  $\xi = \rho/a$  and

$$\mathcal{A}(\xi) = \left[ 2\xi - 2\sqrt{1+\xi^2} + \ln\left(\frac{\sqrt{1+\xi^2}+1}{\sqrt{1+\xi^2}-1}\right) \right]. \quad (23)$$

The effective Hamiltonian now reads

$$H_{\text{eff}} = \sum_{i=1}^2 \left[ h_i + \frac{\pi^2 \hbar^2 n_{z_i}^2}{2m^* a^2} \right] + V_{\text{int}}^{\text{eff}}, \quad (24)$$

where the term  $h_i$  is determined by Eq.(2) and we use Eq.(B2) for the contribution of the vertical confinement. In contrast to the parabolic potential, here  $V_{\text{int}}^{\text{eff}}$  does not depend on the quantum numbers  $n_{z_i}$ . In order to replace  $V_{\text{int}}^{\text{eff}} \rightarrow V_C^{\text{eff}}$  we must define the effective charge. Similar to the previous case, the effective charge is the mean value  $\langle \rho V_{\text{int}}^{\text{eff}}(\rho) \rangle$  in the Fock-Darwin states. For the lowest states with different  $m$  we obtain

$$k_{\text{eff}} = k \frac{2b^{|m|+1}}{|m|!} \int_0^\infty e^{-b\xi^2} \xi^{2|m|+2} \mathcal{A}(\xi) d\xi, \quad (25)$$

where  $b = \mu\Omega a^2/\hbar$ .

### C. Triangular well

Let us consider the well potential characterized by an infinitely high barrier for  $z < 0$  and a linear potential  $V_z(z) = eFz$  for  $z > 0$ ; the product of the electron charge  $e$  and an electric field  $F$  is assumed to be positive:

$$V_z(z) = \begin{cases} \infty, & z < 0 \\ eFz, & z \geq 0 \end{cases}. \quad (26)$$

This potential is a simple realistic description of the potential well at doped heterojunction or/and in the case when an external voltage is applied to the (top and bottom) electrodes of the sample in which the dot is created.

By means of the relation Eq.(C6) (see Appendix C) between the coordinates  $z_i$  and the angle variables  $\theta_{z_i}$ , for the case when both electrons occupy the same energy level  $\varepsilon$ , the effective Coulomb term is

$$V_{\text{int}}^{\text{eff}} = \frac{1}{\pi^2} \int_0^\pi d\theta_{z_1} \int_0^\pi d\theta_{z_2} V_C(\rho, z) \quad (27) \\ = k \int_0^1 d\tilde{\theta}_1 \int_0^1 d\tilde{\theta}_2 [\rho^2 + z_m^2 (\tilde{\theta}_1 - \tilde{\theta}_2)^2 (2 - \tilde{\theta}_1 - \tilde{\theta}_2)^2]^{-1/2} \\ = \frac{k}{z_m} \int_{-1}^0 d\xi_1 \int_{-\xi_1-2}^{\xi_1} d\xi_2 (\xi_3^2 + \xi_1^2 \xi_2^2)^{-1/2} = \frac{k}{z_m} \mathcal{B}(\xi_3),$$

where  $\xi_1 = \tilde{\theta}_1 - \tilde{\theta}_2$ ,  $\xi_2 = \tilde{\theta}_1 + \tilde{\theta}_2 - 2$ ,  $\xi_3 = \rho/z_m$ ,  $z_m = \varepsilon/eF$  and  $\tilde{\theta}_i \equiv \theta_{z_i}/\pi$ .

According to Eq.(C7), the lowest ( $n_z = 1$ ) energy level in the triangular potential is  $\varepsilon_1 = c_1(\hbar eF/\sqrt{2m^*})^{2/3}$ , where  $c_1 = (9\pi/8)^{2/3} \approx 2.32$ . The parameters can be selected to ensure the corresponding wave function (the Airy function, the first zero of this function occurs at  $c_1 = 2.338$ ; see, for example, Ref.13) will be extended until the desired length in the vertical direction. Thus, in the adiabatic approximation the effective Hamiltonian has the form

$$H_{\text{eff}} = H_0 + 2\varepsilon_1 + V_{\text{int}}^{\text{eff}}(\rho), \quad (28)$$

where the term  $H_0$  is defined in subsection II A. As above, we replace  $V_{\text{int}}^{\text{eff}} \rightarrow V_C^{\text{eff}}$  and calculate the effective charge. For the states with  $n_\rho = 0$  (the Fock-Darwin

states for the relative motion) we obtain the effective charge (see Eq.(7))

$$k_{\text{eff}} = k \frac{2b^{|m|+1}}{|m|!} \int_0^\infty d\xi_3 e^{-b\xi_3^2} \xi_3^{2|m|+2} \mathcal{B}(\xi_3), \quad (29)$$

where  $b = \mu\Omega z_m^2/\hbar$  and  $z_m = \varepsilon_1/eF$ . We recall that the parameter  $z_m$  is the distance between turning points. It is similar to the parameter  $a$  in the square well potential. The integral over the variable  $\xi_2$  in the expression for  $\mathcal{B}$  (Eq.(27)) can be evaluated analytically but the other two in Eqs.(27) and (29) must be calculated numerically.

#### IV. DISCUSSION OF RESULTS

In Fig. 2 we present results for the effective charge (ratio  $k_{\text{eff}}/k$ ), calculated for the lowest states ( $n_\rho = n_z = 0$ ) with different  $m$ , with the aid of: a)Eq.(17) for the parabolic confinement as a function of the ratio  $\Omega/\omega_z$  (see Fig. 2(a)); b)Eq.(25) and Eq.(29) for the square and triangular well potentials, respectively, as a function of the variable  $b$  (see Fig. 2(b)). These results evidently demonstrate that the inclusion of the vertical dynamics reduces the Coulomb interaction. In all considered models for the vertical confinement this effect affects strongly quantum states with small values of the quantum number  $m$ . Such states are major participants in the ground state transitions at small and intermediate values of the magnetic field. Therefore, the attenuation of the Coulomb interaction due to the sample thickness may explain the disagreement between experimental data and predictions upon the position of the singlet-triplet transitions based on calculations with the 2D Coulomb potential (see below). In other words, the 2D calculations (with the charge  $k$ ) overestimate the electron correlations in two-electron QDs.

Although the results for the effective charge in the parabolic potential (adiabatic approach) (see Fig.2a) are slightly different in comparison with those of the hard potentials, a general trend for this charge determined by the magnetic field is similar (compare Figs.2a,b). Notice that the magnitude of the ratio and its evolution with the increase of the magnetic field are almost the same in the square and triangular potentials (see Fig.2b). In contrast to the plain quantum-mechanical averaging procedure (see Eqs.(18-20)) in the adiabatic approach (see Eq.(17)) the Coulomb interaction (the ratio  $k_{\text{eff}}/k$ ) is reduced stronger (see below).

To elucidate the quality of the adiabatic approach we use the 3D axially symmetric oscillator model with the lateral ( $\hbar\omega_0 = 3\text{meV}$ ) and the vertical ( $\hbar\omega_z = 12\text{meV}$ ) confinements and compare results for energy levels in 2D, 3D and the effective charge (adiabatic) approximations. For a numerical analysis of spectral properties we choose the effective mass  $m^* = 0.067m_e$ , the relative dielectric constant of a semiconductor  $\varepsilon_r = 12$  and  $|g^*| = 0.44$  (bulk GaAs values). In all three approximations we solve

the eigenvalue problem by means of exact diagonalization of the corresponding Hamiltonian in the Fock-Darwin basis. We recall that in this basis the Coulomb matrix elements are given in analytical form (cf [12]). One observes a remarkable agreement between results for the 3D and the effective charge approximations (see Fig. 3). In the 2D approximation the Coulomb interaction is much stronger and, consequently, the evolution of levels with the magnetic field as well as their absolute values are different from those of the 3D approximation.

To illuminate the key advantage of the effective charge concept it is noteworthy to analyze the available experimental data [7] within various approaches. To this aim we will compare the results of calculations of the additional energy  $\Delta\mu = \mu(N) - \mu(N-1)$  [4, 5] in the 2D approximation (with the effective Coulomb interaction) and in the 3D approach with a full Coulomb interaction. Here, the chemical potential of the dot  $\mu(N) = E(N) - E(N-1)$  is given by the ground-state energy of the dot  $E(N)$  with  $N$  and  $N-1$  electrons. To conduct this study, one needs to estimate the vertical confinement frequency  $\hbar\omega_z$  in a real sample. The simplest approach is to use the parabolic model for the vertical confinement in the layer of thickness  $a$  (see Fig.1).

The thickness of QDs is much smaller in comparison with the lateral extension. Therefore, the vertical confinement  $\hbar\omega_z$  is much stronger than the lateral confinement  $\hbar\omega_0$  and this fact is, usually, used to justify a 2D approach for the study of QDs. However, there is a nonzero contribution from the vertical dynamics, since the energy level available for each of the noninteracting electrons in the  $z$  direction is  $\varepsilon = \hbar\omega_z(n_z + 1/2)$ . For the lowest state  $n_z = 0 \Rightarrow \varepsilon_1 = \frac{1}{2}\hbar\omega_z$ . By dint of the condition  $V_z(\pm z_m) \equiv m^*\omega_z^2 z_m^2/2 = \varepsilon_1$  one defines the turning points:  $z_m = \sqrt{\hbar/(m^*\omega_z)}$  (see Fig.1). We assume that the distance between turning points should not exceed the layer thickness, i.e.,  $2z_m \leq a$ . From this inequality it follows that the lowest limit for the vertical confinement in the layer of thickness  $a$  is

$$\hbar\omega_z \geq \frac{4\hbar^2}{m^*a^2} \quad (30)$$

or  $b > 2\Omega/\omega_z$ . For typical GaAs samples with the thickness  $a$  between 10 nm and 20 nm this estimation gives the minimal value for  $\hbar\omega_z$  between 45 meV and 11 meV, respectively. These estimations provide a genuine cause for the use of the adiabatic approach in case of QDs, since  $T_z (= 2\pi/\omega_z) \ll T_0 (= 2\pi/\omega_0)$ .

Using the "experimental" values for the lateral confinement and the confinement frequency  $\omega_z$  as a free parameter, we reproduced successfully with the value  $\hbar\omega_z = 8\text{meV}$  and  $|g^*| = 0.3$  the positions of kinks in the additional energy for a two-electron QD (see Fig.4a)

$$\Delta\mu = E_{\text{rel}} - E(1) + E_{\text{spin}} \quad (31)$$

in all three samples [7] in the 3D axially symmetric oscillator model [10]. Here,  $E_{\text{rel}} = \langle H_{\text{rel}} \rangle$  is the relative

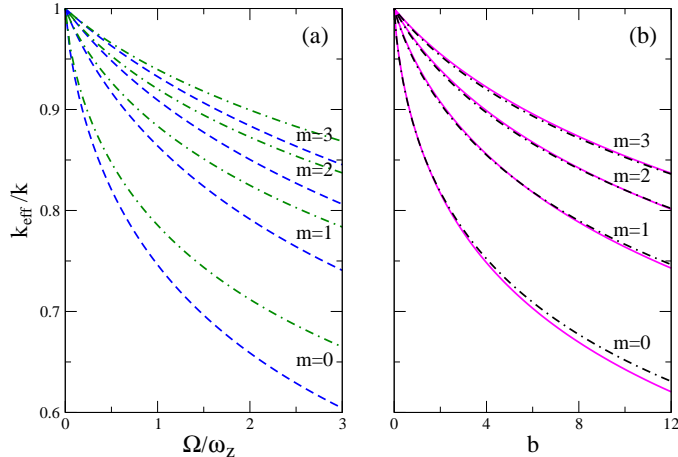


FIG. 2: (Color online) The ratio  $k_{\text{eff}}/k$  for the lowest states with different  $m$  for the vertical confinement approximated by: (a) the parabolic potential; (b) the hard wall (square/triangular well) potentials. (a) The results obtained in the adiabatic approximation and by means of the plain quantum-mechanical averaging procedure (see subsection III A) are connected by dashed (blue) and dotted-dashed (green) lines, respectively. (b) The results for the square and triangular well are connected by solid (pink) and dotted-dashed lines, respectively.

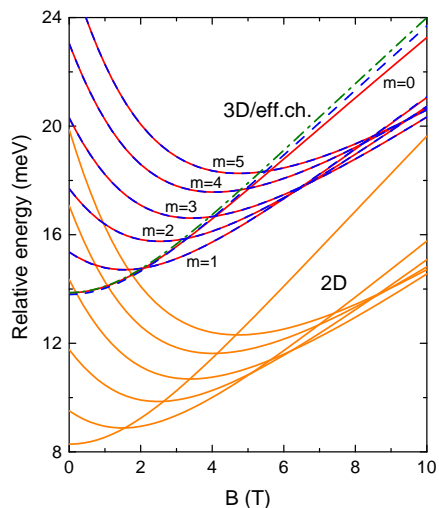


FIG. 3: Lowest energy levels (only the relative motion is considered) of the two-electron QD with fully parabolic potential. The results of the 2D, the 3D and the effective charge (adiabatic) approximations are connected by solid (orange), solid (red), and dashed (blue) lines, respectively. The result of the plain quantum-mechanical averaging for the  $m = 0$  level ( $k_{\text{eff}} = \langle \langle \rho V_C \rangle \rangle$ ) is connected by the dotted-dashed (green) line.

energy,  $E(1) = \hbar\omega_0 + \hbar\omega_z/2$  is a single-electron energy and the Zeeman energy  $E_{\text{spin}} = -|g^*|\mu_B[1 - (-1)^m]B/2$  is zero for the singlet states. Note that it was found from the Zeeman splitting at high magnetic field that  $|g^*| = 0.3$  [18]. While at small magnetic field the results for  $|g^*| = 0.44$  and  $|g^*| = 0.3$  are similar, the latter value provides the best agreement between the full 3D

calculations and the experimental data.

We recall that in the 2D approach used by Nishi *et al.* [7] one encounters the problem of the correct interpretation of the experimental data (see Fig.4a, a plain lateral confinement  $\hbar\omega_0 = 2.9$  meV). In the effective charge approximation the vertical confinement is taken into account with the aid of  $k_{\text{eff}}$  in the 2D effective Hamiltonian. The remarkable accord between the predictions based on the results of Section III A and the observation confirms the validity of the suggested concept (see Fig. 4). We stress that the effective charge approximation facilitates the calculations providing the same results as the full 3D calculations.

Notice that the results based upon the adiabatic approximation are in a better agreement with the full 3D calculations in contrast to those obtained with the aid of the plain quantum-mechanical averaging procedure for  $k_{\text{eff}} = \langle \langle \rho V_C(\rho, z) \rangle \rangle$ . As discussed in Section II B, the adiabatic approach is based on the effective separation of fast (vertical) and slow (lateral) dynamics with subsequent averaging procedure. In contrast, the plain quantum-mechanical averaging represents a type of perturbation theory based upon the first order contribution with respect to the ratio  $z/\rho$  only. The higher order term may improve the agreement at small magnetic field, since the vertical dynamics is non negligible and affects the lateral dynamics. The increase of the quantum number  $m$ , caused by the increase of the magnetic field strength, reduces the orbital motion of electrons in the vertical direction. The larger is  $m$  the stronger is the centrifugal force, which induces the electron localization in a plane, and, therefore, the lesser is importance of the vertical electron dynamics. In the limit of strong magnetic field (large  $m$ ) the dot becomes more of a "two-dimensional"

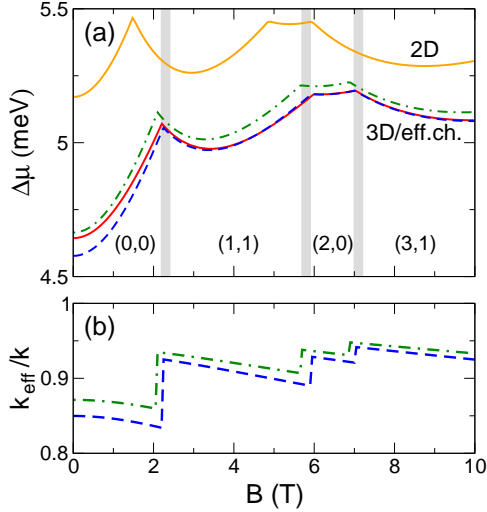


FIG. 4: (Color online) (a) The additional energy  $\Delta\mu$  as a function of the magnetic field in the parabolic model for a two-electron QD. The results of calculations with a lateral confinement only (the 2D approach,  $\hbar\omega_0 = 2.9$  meV,  $|g^*| = 0.3$ ) and full 3D approach [10] ( $\hbar\omega_z = 8$  meV) are connected by solid (orange) and (red) lines, respectively. The vertical grey lines indicate the position of the experimental crossings between different ground states [7]. Ground states are labeled by  $(m, S)$ , where  $m$  and  $S$  are the quantum numbers of the operators  $l_z$  and the total spin, respectively. The results based upon the adiabatic approximation, Eq.(17), and the plain quantum-mechanical averaging procedure, Eq.(19), are connected by dashed (blue) and dot-dashed (green) lines, respectively. (b) The ratio  $k_{\text{eff}}/k$  as functions of the magnetic field based on Eq.(17) and the plain quantum-mechanical averaging, Eq.(19) are connected by dashed (blue) and dotted-dashed (green) lines, respectively.

system. This explains the improvement of the accuracy of the plain quantum-mechanical averaging procedure at large  $m$ , i.e., for the ground states at high magnetic fields.

The results of different averaging procedures indicate that the accuracy of the methods depends, indeed, on the quality of the separation between the lateral ( $\rho$ ) and vertical ( $z$ ) components of the Coulomb interaction, with further averaging over them. We recall that the essence of the "removal of resonances" technique based on the action-angle variables [11] is the identification of adiabatic invariants, i.e., approximately conserved integrals of motion. The averaging of the Hamiltonian over the fast variables is a next step within this technique. In our case such an invariant is the action  $J_z$ , which is approximately conserved due to large difference in a time scale between fast vertical ( $z$ ) and slow lateral ( $xy$ ) dynamics. Therefore, the integration over fast variable (angle) is well justified in this case. As it was pointed out above, at small magnetic field a plain quantum-mechanical procedure, which reduces to a variant of the first order perturbation theory, is less justified. In fact, the effective potential obtained from the plain quantum-mechanical

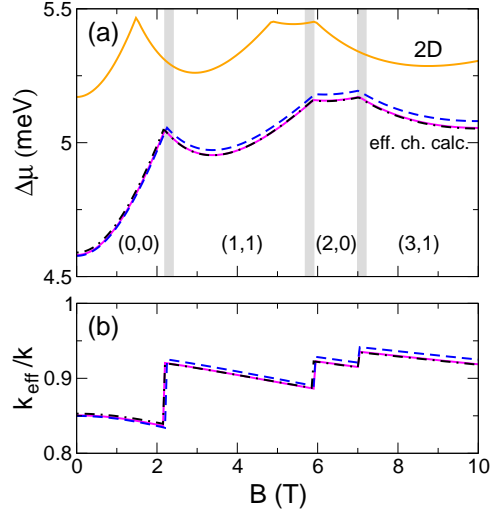


FIG. 5: (Color online) (a) The magnetic dependence of the additional energy  $\Delta\mu$  for a two-electron QD with the lateral confinement  $\hbar\omega_0 = 2.9$  meV and  $|g^*| = 0.3$ . The results of the pure 2D approach are connected by the solid (orange) line. The results of the adiabatic approach (effective charge calculations) are connected: by the dashed (blue) line for the parabolic model ( $\hbar\omega_z = 8$  meV); by the solid (pink) line for the square well model ( $a = 32.5$  nm); by the dotted-dashed (black) line for the triangular well model ( $F = 220$  kV/m). See the text for details. The vertical grey lines indicate the position of the experimental crossings between different ground states labeled by  $(m, S)$  [7]. (b) The ratio  $k_{\text{eff}}/k$  for three different approximations of the vertical confinement as a function of the magnetic field.

procedure is significantly stronger at small distances between two electrons (see Appendix A). In turn, in this case the effective coupling between the vertical and lateral confinements is stronger, which indicates a less efficiency of the separation procedure.

The positions of the singlet-triplet transitions in the same sample can be reproduced as well with a vertical confinement approximated by the square (Section III B) and the triangular (Section III C) potentials. It appears from the behavior of the effective charge for the considered models of the vertical confinement (see Fig. 2) that one obtains equivalent results if the ratio  $\kappa = b/(\Omega/\omega_z)$  between the distance  $b$  in the square/triangular well and the parabolic variable  $\Omega/\omega_z$  is  $\kappa \sim 4$ . Note that this conclusion is independent on the particular value of the vertical confinement in the parabolic model, since this parameter enters in the calculations of the  $k_{\text{eff}}$  through the ratio  $\Omega/\omega_z$ .

Within the square well model the best agreement with the experimental data is obtained for  $a \approx 32.5$  nm (see Fig.5). In virtue of the definition  $b = \mu\Omega a^2/\hbar$  we have

$$\kappa = b/\left(\frac{\Omega}{\omega_z}\right) = \frac{m^* a^2 \hbar \omega_z}{2\hbar^2}. \quad (32)$$

Using the above value for  $a$  and  $\hbar\omega_z = 8$  meV which

provides the equivalent result in the parabolic model, we obtain  $\kappa = 3.715$ . Indeed, this estimation is close to the one extracted from Fig.2 which is independent on the specific parameters of the QD.

Similar agreement with the experimental data is obtained by means of the triangular well potential ( $b = \mu\Omega z_m^2/\hbar$ ) for the electric field  $F \approx 220$  kV/m which corresponds to  $z_m \approx 32.1$  nm (see Fig. 5). Note that in all considered models the effective charge  $k_{\text{eff}}$  of the Coulomb interaction changes with the increase of the magnetic field in a similar way (see Fig. 5) producing approximately the equivalent effect in all three cases. At very large magnetic fields the effective charge approaches almost the value  $k_{\text{eff}} \approx 0.95k$ .

Finally, a remark is in order. For the sake of illustration we have used only  $k_{\text{eff}}$  for the lowest basis states ( $n_\rho = n'_\rho = 0$ ) with different  $m$ . However, even for the ground state calculations with the aid of the exact diagonalization, the interaction matrix elements  $k_{\text{eff}} \langle n'_\rho, m | \rho^{-1} | n'_\rho, m \rangle$  with  $n_\rho, n'_\rho \geq 0$  have been taken into account. Namely, the diagonalization is performed using the interaction matrix elements up to  $n_\rho, n'_\rho = 10$ . Obviously, the accuracy of the method would improve if one calculates the 'effective charge matrix elements'  $k_{n_\rho, n'_\rho}^{(m)} = \langle n'_\rho, m | \rho V_{\text{int}}^{\text{eff}} | n'_\rho, m \rangle$  for each interaction matrix element. However, in this case the procedure would lose the simplicity and become impractical. Fortunately, from the comparison of the present results with exact 3D calculations we found that for the analysis of the ground state properties it is sufficient to use only the elements  $k_{0,0}^{(m)} \equiv k_{\text{eff}}^{(m)}$ , even for the interaction matrix elements with  $n_\rho, n'_\rho \geq 0$ .

## V. SUMMARY

We developed the effective charge approach taking full account of the thickness of two-electron quantum dots. Our approach is based on the adiabatic approximation where the full 3D dynamics of two interacting electrons is separated by means of action-angle variables on the independent vertical motion and the lateral dynamics described by the effective 2D Hamiltonian. The separation is reached due to different time scales in the vertical (fast) and lateral (slow) dynamics and it is well justified in all types of QDs (vertical and lateral). As a result, one must solve only the Schrödinger equation for the 2D effective Hamiltonian where the full charge  $k$  is replaced by  $k_{\text{eff}}$  (see Eqs.(7), (10)). The eigenvalue problem was solved by means of the exact diagonalization of the effective 2D Hamiltonian in the Fock-Darwin basis. To demonstrate the feasibility of the effective charge approach, we considered three different models for the vertical confinement: the parabolic, the square and triangular well potentials. The use of the parabolic potential simplifies the analysis due to the Kohn theorem which results in the analytical expression for the effective charge, Eq.(17). For the

square and triangular well potentials we obtained expressions for the effective charge Eqs.(25),(29), respectively, that can be easily calculated numerically.

The value of the effective charge depends on the (good) quantum number  $m$  of the correlated state (see Fig.2). We established a scaling factor, Eq.(32), between the variables used in the parabolic and the square/triangular well potentials. Taking into account this factor, we found that the effective charge (screening of the Coulomb interaction) affects quantum states for all potentials in a similar way. The screening due to the sample thickness is especially strong for quantum states with small values of the quantum number  $m$ . We recall that these states determine the structure of the ground state transitions at small and intermediate values of the magnetic field. Therefore, the screening provides a consistent way to deal with the effect of the thickness upon the position of the singlet-triplet transitions. In particular, the screening should be taken into account for the analysis of evolution of the energy difference between singlet and triplet states in the magnetic field. This energy is considered to be important for analysis of the entanglement and concurrence in QDs (cf [19]).

The comparison of the results with available experimental data [7] demonstrates a remarkable agreement and lends support to the validity of the approach. Being important for the states with small quantum number  $m$ , the screening of the Coulomb interaction becomes small for the states with large  $m$ , which dominate in the low-lying spectrum at large magnetic fields. On the other hand, these states cause strong centrifugal forces which induce the electron localization in a plane. In turn, the stronger is the magnetic field the less important is the vertical confinement. It follows that the 2D bare Coulomb potential becomes reliable in 2D approaches for the analysis of the ground state evolution of QDs only at very large magnetic fields.

Thus, the 2D calculations with a bare Coulomb interaction (with the charge  $k$ ) overestimate the electron correlations in two-electron QDs at small and intermediate values of the magnetic field. One may induce that similar conclusion could be valid for QDs with more than two electrons. Notice, however, that the confining frequency in the lateral plane decreases with the increase of the electron number  $N > 2$  in exact 3D calculations at fixed vertical confinement [20], making QDs to be more of a two-dimensional system. A thorough analysis of our approach for  $N > 2$  is left for the future.

## Acknowledgments

This work was partly supported by Project No 141029 of Ministry of Science and Environmental Protection of Serbia, by Grant No. FIS2005-02796 (MEC, Spain) and RFBR Grant No. 08-02-00118 (Russia).



## APPENDIX A: EFFECTIVE INTERACTION POTENTIAL FOR THE PARABOLIC VERTICAL CONFINEMENT AT $n_z = 0$

The effective electron-electron interaction potential is obtained by averaging the Coulomb term  $V_C(\rho, z)$  in the  $z$ -direction

$$V_{\text{int}}^{\text{eff}}(\rho) = \int w(z) V_C(\rho, z) dz, \quad (\text{A1})$$

where  $w(z)$  is the corresponding weight function. By dint of the quantum-mechanical averaging one obtains the effective potential

$$V_{\text{int}}^{\text{eff(qm)}}(\rho) = \int_{-\infty}^{\infty} |\psi_{n_z}(z)|^2 V_C(\rho, z) dz, \quad (\text{A2})$$

while in the adiabatic approach we have the effective potential

$$\begin{aligned} V_{\text{int}}^{\text{eff(ad)}}(\rho) &= \frac{1}{\pi} \int_{-\pi/2}^{\pi/2} V_C(\rho, z(\theta_z)) d\theta_z \\ &= \frac{1}{\pi} \int_{-z_0}^{z_0} \left( \frac{d\theta_z}{dz} \right) V_C(\rho, z) dz. \end{aligned} \quad (\text{A3})$$

For  $n_z = 0$ , we have for the quantum-mechanical weight function

$$w_{\text{qm}} \equiv |\psi_{n_z=0}(z)|^2 = \frac{e^{-(z/z_0)^2}}{\sqrt{\pi} z_0}, \quad (\text{A4})$$

while, by virtue of Eq.(12) and  $J_z = \hbar/2$ , one obtains for the adiabatic weight function

$$w_{\text{ad}} \equiv \pi^{-1} (d\theta_z/dz) = \frac{1}{\pi z_0 \sqrt{1 - (z/z_0)^2}}, \quad (\text{A5})$$

where  $z_0 = \sqrt{\hbar/\mu\omega_z}$ . As it can be seen from Fig. 6(a) the weight functions  $w_{\text{qm}}$  (solid line) and  $w_{\text{ad}}$  (dashed line) are completely different and, therefore, one may expect different contributions of the  $z$ -motion in the effective 2D potential, i.e., a different  $\rho$ - $z$  coupling.

By dint of the definition  $V_C = k/(\rho^2 + z^2)^{1/2}$  and Eqs.(A4),(A5) one obtains for the effective interaction potentials (Eqs.(A2),(A3)):

$$V_{\text{int}}^{\text{eff(qm)}}(\rho) = \frac{k}{\sqrt{\pi} z_0} e^{\rho^2/2z_0^2} K_0\left(\frac{\rho^2}{2z_0^2}\right), \quad (\text{A6})$$

$$V_{\text{int}}^{\text{eff(ad)}}(\rho) = \frac{2k}{\pi\rho} K\left(-\frac{z_0^2}{\rho^2}\right), \quad (\text{A7})$$

where  $K_0$  and  $K$  are the the modified Bessel function of the 2nd kind and the complete elliptic integral of the first kind, respectively.

Although the potential  $V_C^{\text{eff(qm)}}$  is akin to the potential  $V_{\text{int}}^{\text{eff(ad)}}$ , the ratio  $R = V_{\text{int}}^{\text{eff(ad)}}/V_{\text{int}}^{\text{eff(qm)}} < 1$  at  $0 < \rho < \sqrt{2}z_0$  (see Fig. 6(b)). We recall that for the

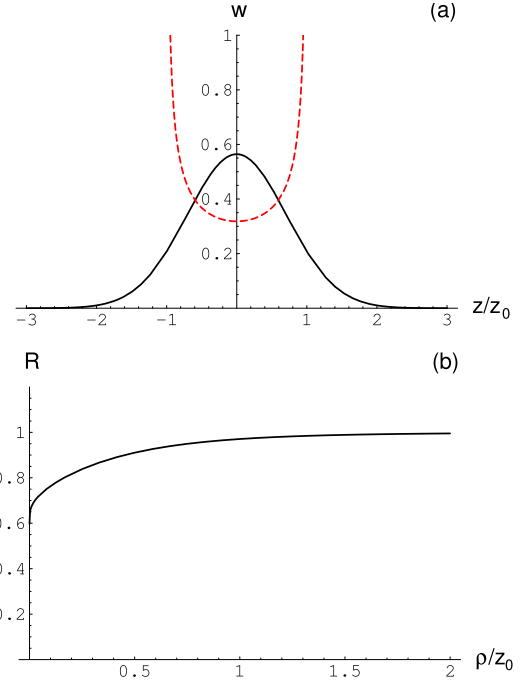


FIG. 6: (Color online)(a) The weight functions  $w_{\text{qm}}$  (solid line),  $w_{\text{ad}}$  (dashed line) and (b) the ratio  $R = V_{\text{int}}^{\text{eff(ad)}}/V_{\text{int}}^{\text{eff(qm)}}$  for the parabolic vertical confinement.

lowest limit of the sample thickness  $a = 2z_m = \sqrt{2}z_0$  (see Fig.1). In other words, when electrons are close to each other (for  $\rho < a$ ), the effective quantum-mechanical potential is significantly stronger than the adiabatic one. At distances between electrons  $\rho > a$  two potentials reach each other asymptotically ( $R \rightarrow 1$ ).

## APPENDIX B: ACTION-ANGLE VARIABLES IN THE ONE-DIMENSIONAL SQUARE WELL POTENTIAL

If  $\varepsilon$  is the energy of a particle of the mass  $m^*$  moving in the infinite square well potential (21), its momentum  $p_z = \pm\sqrt{2m^*\varepsilon}$  change the sign at the turning points  $\pm a/2$ . In this case the action variable is

$$J_z = \frac{1}{\pi} \int_{-a/2}^{a/2} p_z dz = \frac{a}{\pi} \sqrt{2m^*\varepsilon}. \quad (\text{B1})$$

Accordingly, the energy expressed in terms of  $J_z$  is  $\varepsilon = \pi^2 J_z^2 / (2m^* a^2)$ . By dint of the semiclassical quantization condition  $J_z = \hbar(n_z + 1)$  ( $n_z = 0, 1, 2, \dots$ ), one obtains energy levels for a particle moving in the potential (21). The value 1 in this condition is a Maslov index (cf [17]). It is convenient to define  $n_z \rightarrow n_z + 1$ . Finally, one has

$$\varepsilon = \frac{\hbar^2}{2m^*} \left( \frac{\pi n_z}{a} \right)^2, \quad n_z = 1, 2, \dots \quad (\text{B2})$$

Integrating equation  $m^* \dot{z} = p_z$ , from the condition  $z(T/4) = a/2$  (for  $-a/2 < z < a/2$ ) one can define the period  $T = 2a\sqrt{m^*/2\varepsilon}$ . It follows that the angle variable  $\theta_z$  has the form

$$\theta_z = \omega_z t = \frac{2\pi}{T} t = \frac{\pi}{a} \sqrt{\frac{2\varepsilon}{m^*}} t = \frac{\pi}{a} z. \quad (\text{B3})$$

### APPENDIX C: ACTION-ANGLE VARIABLES IN A TRIANGULAR WELL POTENTIAL

For a particle moving with energy  $\varepsilon$  in the triangular well potential (26) the turning points are  $z = 0$  and  $z = z_m$ . In virtue of equation  $p_z \equiv \pm\sqrt{2m^*(\varepsilon - eFz)} = 0$  one defines the variable  $z_m = \varepsilon/eF$  and, respectively, the action variable

$$J_z = \frac{1}{\pi} \int_0^{z_m} p_z dz = \frac{2\sqrt{2m^*}\varepsilon^{3/2}}{3\pi eF}. \quad (\text{C1})$$

In turn, the energy expressed in terms of  $J_z$  is

$$\varepsilon = [3\pi J_z eF / \sqrt{8m^*}]^{2/3}. \quad (\text{C2})$$

From Eq.(C2) one can define the angle variable

$$\theta_z = \omega_z t = \frac{\partial \varepsilon}{\partial J_z} t = \frac{\pi eF}{\sqrt{2m^*}\varepsilon} t \quad (\text{C3})$$

and, consequently, the period  $T = 2\pi/\omega_z = 2\sqrt{2m^*}\varepsilon/eF$ . Integrating equation  $m^* \dot{z} = p_z$ , one obtains

$$t = m^* \int_0^z \frac{dz}{p_z} = \frac{\sqrt{2m^*}\varepsilon}{eF} \left( 1 - \sqrt{1 - \frac{eF}{\varepsilon} z} \right), \quad (\text{C4})$$

for  $0 \leq z \leq z_m$  or

$$z = \sqrt{\frac{2\varepsilon}{m^*}} t - \frac{eF}{2m^*} t^2, \quad 0 \leq t \leq T/2. \quad (\text{C5})$$

By dint of equation  $t = \theta_z/\omega_z$ , it is useful to establish the relation between the coordinate  $z$  and the variable  $\theta_z$

$$z = z_m \left[ 2\frac{\theta_z}{\pi} - \left( \frac{\theta_z}{\pi} \right)^2 \right], \quad 0 \leq \theta_z \leq \pi. \quad (\text{C6})$$

For the triangular potential one has the semiclassical quantization condition  $J_z = \hbar(n_z + 3/4)$ , where  $n_z = 0, 1, 2, \dots$  and the Maslov index = 3/4. Redefining  $n_z \rightarrow n_z - 1$ , one obtains the semiclassical energy levels from Eq.(C2)

$$\varepsilon_{n_z} = c_{n_z} \left[ \frac{(eF\hbar)^2}{2m^*} \right]^{1/3}, \quad c_{n_z} = \left[ \frac{3}{2}\pi(n_z - \frac{1}{4}) \right]^{2/3} \quad (\text{C7})$$

with  $n_z = 1, 2, \dots$

- 
- [1] S. Kais, D. R. Herschbach, and R. D. Levine, *J. Chem. Phys.* **91**, 7791 (1989).
- [2] M. Taut, *Phys. Rev. A* **48**, 3561 (1993).
- [3] M. Taut, *J. Phys. A* **27**, 1045 (1994).
- [4] R. C. Ashoori, H. L. Stormer, J. S. Weiner, L. N. Pfeiffer, K. W. Baldwin, and K. W. West, *Phys. Rev. Lett.* **71**, 613 (1993).
- [5] L. P. Kouwenhoven, D. G. Austing, and S. Tarucha, *Rep. Prog. Phys.* **64**, 701 (2001).
- [6] S. M. Reimann and M. Manninen, *Rev. Mod. Phys.* **74**, 1283 (2002).
- [7] Y. Nishi, Y. Tokura, J. Gupta, G. Austing, and S. Tarucha, *Phys. Rev. B* **75**, 121301(R) (2007).
- [8] M. Rontani, F. Rossi, F. Manghi, and E. Molinari, *Phys. Rev. B* **59**, 10165 (1999).
- [9] N. A. Bruce and P. A. Maksym, *Phys. Rev. B* **61**, 4718 (2000).
- [10] R. G. Nazmitdinov and N. S. Simonović, *Phys. Rev. B* **76**, 193306 (2007).
- [11] A. J. Lichtenberg and M. A. Liberman, *Regular and Stochastic Motion* (Springer, New York, 1983).
- [12] L. Jacak, P. Hawrylak, and A. Wojs, *Quantum Dots* (Springer, Berlin, 1998).
- [13] L. D. Landau and E. M. Lifshits, *Quantum Mechanics*, Vol.III (Pergamon Press, Oxford, 1977).
- [14] W. Kohn, *Phys. Rev.* **123**, 1242 (1961).
- [15] M. Abramowitz and I. A. Stegun, *Handbook of Mathematical Functions with Formulas, Graphs, and Mathematical Tables Tenth Printing* National Bureau of Standards, Applied Mathematics Series 55, (U.S. Government Printing Office, Washington, DC, 1972) p.590.
- [16] I. S. Gradshteyn and I. M. Ryzhik, *Table of Integrals, Series, and Products Fifth Edition* (Academic Press, NY, 1994) pp.898,1096.
- [17] M. Brack and R. K. Bhaduri, *Semiclassical Physics* (Addison-Wesley, Reading, 1997).
- [18] Y. Nishi, P. A. Maksym, D. G. Austing, T. Hatano, L. P. Kouwenhoven, H. Aoki, and S. Tarucha, *Phys. Rev. B* **74**, 033306 (2006).
- [19] D. M. Zumbühl, C. M. Marcus, M. P. Hanson, and A. C. Gossard, *Phys. Rev. Lett.* **93**, 256801 (2004).
- [20] D. V. Melnikov and J-P. Leburton, *Phys. Rev. B* **73**, 085320 (2006).